Algebraic Depletion Interactions in Two-Temperature Mixtures

Pascal Damman,[1,*] Vincent Démery,[2,3,†] Guillaume Palumbo,[1] and Quentin Thomas[1]
[1]Laboratoire Interfaces & Fluides Complexes, Université de Mons, 20 Place du Parc, B-7000 Mons, Belgium
[2]Gulliver, CNRS, ESPCI Paris, PSL Research University, 10 rue Vauquelin, 75005 Paris, France
[3]ENS de Lyon, CNRS, Laboratoire de Physique, F-69342 Lyon, France

(Received 20 June 2024; revised 21 October 2024; accepted 18 November 2024; published 27 December 2024)

The phase separation that occurs in two-temperature mixtures, which are driven out of equilibrium at the local scale, has been thoroughly characterized, but much less is known about the depletion interactions that drive it. Using numerical simulations in dimension 2, we show that the depletion interactions extend beyond two particle diameters in dilute systems, as expected at equilibrium, and decay algebraically with an exponent -4. Solving for the N-particle distribution function in the stationary state, perturbatively in the interaction potential, we show that algebraic correlations with an exponent $-2d$ arise from triplets of particles at different temperatures in spatial dimension d. Finally, simulations allow us to extend our results beyond the perturbative limit.

DOI: 10.1103/PhysRevLett.133.267103

At equilibrium, coupling two objects to a critical field induces an algebraic effective interaction between these objects. The field may be the electromagnetic field, as in the Casimir effect [1,2], or the density fluctuations in a binary mixture close to its critical point [3–5]. In the latter case, inducing such interactions requires the fine tuning of the temperature [5]. Out of equilibrium, algebraic correlations and the effective interactions that they induce are much more frequent and usually do not require fine tuning. They arise, for instance, in driven systems, such as an electrolyte or a binary colloidal mixture under an electric field [6–10]. Transient algebraic interactions can also arise during the relaxation following a temperature quench [11,12]. Finally, active systems can induce interactions [13], which may decay algebraically for asymmetric bodies [14,15] or if the active system is flocking [16]. Here, we show that algebraic interactions spontaneously appear in mixtures of particles connected to different thermostats, an out of equilibrium system known to exhibit phase separation [17–19]. This algebraic depletion interaction thus does not require self-propulsion and acts between spherical bodies.

Two-temperature mixtures are now a paradigmatic model to study nonequilibrium phenomena. They are driven out of equilibrium locally, such as active systems, but do not involve self-propulsion; they are thus simpler than the active-passive mixture that they may represent [20–22]. Two-temperature mixtures can also be mapped to systems with nonreciprocal interactions [23,24], which have gained attention recently [25]. The hot and cold particles may phase separate even when the interactions between the particles are purely repulsive and identical, provided that the temperature ratio is large enough [18,19,26], resulting in dense droplets of cold particles coexisting with a dilute gas of hot particles. Grosberg and Joanny provided an analytical prediction for the instability threshold in a dilute system [18], showing that denser systems are easier to phase separate. Recently, McCarthy *et al.* found that the two species may mix again at high density [27].

To understand the phase separation mechanism, it is instructive to consider the depletion interaction between the cold particles that is induced by the hot particles, which is encoded in the pair correlation of the cold particles [19]. In the approach of Grosberg and Joanny, the free energy of the system can be minimized with respect to the density of the hot particles to get an effective free energy functional for the cold particles only [18]. However, this free energy contains only a coarse-grained description of the interaction between the particles, namely the integral of the Mayer function, and does not provide the shape of the effective interaction. An explicit expression of the effective interaction has been obtained in Ref. [26] using the potential of mean force; however, the application of this approach to an out-of-equilibrium system is questionable. Indeed, we will see that generalizing different equilibrium methods to compute the effective interactions in this out-of-equilibrium system leads to different results, similarly to the situation observed with the pressure in a gas of active particles [28].

In this Letter, we investigate the depletion interaction between cold particles that is due to the hot particles in the dilute limit using analytical calculations and numerical simulations. Restricting ourselves to the dilute limit amounts to considering a system of two cold particles and a single hot one. Contrary to two-body problems [18,23], this three-body system cannot be mapped onto an effective

*Contact author: pascal.damman@umons.ac.be
†Contact author: vincent.demery@espci.psl.eu

equilibrium system [29]. We compute the depletion interaction analytically, perturbatively in the interaction strength ϵ. At order ϵ^2, we show that the potential of mean force argument should be corrected by a purely nonequilibrium three-body potential. At order ϵ^3, we find that the three-body potential gives rise to algebraic interactions decaying as r^{-2d} in spatial dimension d. Simulations confirm our analytical results for weak interactions and show that the algebraic decay is still present for strong interactions, allowing us to discuss the dependence of the magnitude of this decay on the interaction potential.

We consider particles with positions $\boldsymbol{x}_i(t)$, connected to thermostats with temperature T_i and obeying an overdamped Langevin dynamics:

$$\dot{x}_i(t) = -\sum_j \nabla V[\boldsymbol{x}_i(t) - \boldsymbol{x}_j(t)] + \sqrt{2T_i}\boldsymbol{\eta}_i(t), \quad (1)$$

where $V(r) = \epsilon U(r)$ is the interaction potential. The vectorial Gaussian white noises $\boldsymbol{\eta}_i$ have a unit variance and are uncorrelated. The particles mobility and the Boltzmann constant have been set to unity. We consider only two species $\alpha \in \{A, B\}$ connected to thermostats T_α. To focus on the interactions induced by the particles B on the particles A, we assume that there are only two A particles $i \in \{1, 2\}$ and a small density ρ of B particles. We expand the pair distribution function of the two A particles $g(r)$ as $g(r) = \exp[-V(r)/T_A][1 + \sum_{n=1}^{\infty} \rho^n g_n(r)]$ [30]. We focus on the first term of the expansion, $g_1(r)$; we denote it $\hat{g}(r)$ and refer to it as the "correlation":

$$\hat{g}(r) = \lim_{\rho \to 0} \frac{e^{V(r)/T_A} g(r) - 1}{\rho}. \quad (2)$$

This order is not affected by the interactions between the B particles, which can render the depletion interaction nonmonotonic [31].

At equilibrium, here when $T_A = T_B = T$, the interaction induced by the B particles can be obtained by integrating the three body distribution $f(\boldsymbol{x}_1, \boldsymbol{x}_2, \boldsymbol{x}_3)$ over the coordinate of the third particle, leading to [32]

$$\hat{g}_{\mathrm{eq}}(r) = (e^{-V/T} - 1) * (e^{-V/T} - 1)(r), \quad (3)$$

where the star denotes the convolution product. In the weak interaction limit $\epsilon \ll T$ it reduces to

$$\hat{g}_{\mathrm{eq}}(r) = \frac{V * V(r)}{T^2} + \mathcal{O}(\epsilon^3). \quad (4)$$

If the potential $U(r)$ has a finite range σ, which represents the diameter of the particles, both the full expression (3) and its weak interaction limit (4) are zero beyond two particle diameters. The same expressions can be recovered using the potential of mean force [30,32].

These arguments can be transposed out of equilibrium, using the fact that an isolated pair of particles (i, j) is in an effective equilibrium at temperature $T_{ij} = (T_i + T_j)/2$ so that its pair correlation is $g_{ij}(r) = \exp[-v_{ij}(r)]$, where $v_{ij}(r) = V(r)/T_{ij}$ [18]. Using the potential of mean force, Ilker and Joanny obtained [26]

$$\hat{g}(r) = \frac{T_B}{T_A}(e^{-V/T_{AB}} - 1) * (e^{-V/T_{AB}} - 1)(r) \quad (5)$$

$$= \frac{T_B}{T_A T_{AB}^2} V * V(r) + \mathcal{O}(\epsilon^3). \quad (6)$$

Alternatively, assuming that the N-particle distribution function is given by $f(\boldsymbol{X}) = \exp\left(-\sum_{\langle ij \rangle} v_{ij}(\boldsymbol{x}_i - \boldsymbol{x}_j)\right)$, where $\boldsymbol{X} = (\boldsymbol{x}_i)_{1 \le i \le N}$, we get [32]

$$\hat{g}(r) = (e^{-V/T_{AB}} - 1) * (e^{-V/T_{AB}} - 1)(r) \quad (7)$$

$$= \frac{V * V(r)}{T_{AB}^2} + \mathcal{O}(\epsilon^3). \quad (8)$$

The temperatures enter differently into the predictions (5) and (7), pointing to the fact that these approaches may not apply out of equilibrium. However, they agree on the form of the depletion interaction, which is the same as the equilibrium one; in particular its range is limited to two particle diameters.

We simulated Eq. (1) numerically [32,33] in spatial dimension $d = 2$ for three different interactions between particles with diameter $\sigma = 1$: harmonic, $U_{\mathrm{harm}}(r) = (1 - r)^2\theta(1 - r)$, θ being the Heaviside function, Gaussian, $U_{\mathrm{Gauss}}(r) = \exp(-6r^2)$, and Weeks-Chandlers-Andersen (WCA), $U_{\mathrm{WCA}}(r) = (r^{-6} - 1)^2\theta(1 - r)$. In order to improve the statistics, we used the same small density ρ of A and B particles. In this situation, an additional depletion interaction is induced by the particles A themselves, so that $\hat{g}(r) = \hat{g}^A(r) + \hat{g}^B(r)$, where $\hat{g}^A(r) = \hat{g}_{\mathrm{eq}}(r)$ [Eq. (3)]. The correlations $\hat{g}(r)$ calculated from simulations with a harmonic interaction, $\epsilon = 10$, $\rho = 0.05$, $T_A = 1$ and different values of T_B are presented in Fig. 1(a). As expected, we observe an increase of the correlation at contact $\hat{g}(1)$ due to the depletion interaction. This increase scales as ϵ^2 with the interaction strength ϵ, as expected from the different theoretical predictions [Fig. 1(b)]. However, in contradiction with the predictions, the depletion interaction extends beyond two diameters as soon as the system departs from equilibrium. Beyond two particle diameters, the radial dependence of the depletion interaction is compatible with an algebraic decay, $\hat{g}(r) = G/r^4$. The prefactor G of the algebraic decay increases with the interaction strength as ϵ^3 for small ϵ and saturates for large values of ϵ, corresponding to the hard sphere limit [Fig. 1(b)]. The effect of the temperature T_B is nonmonotonic: G first increases and then decreases at large

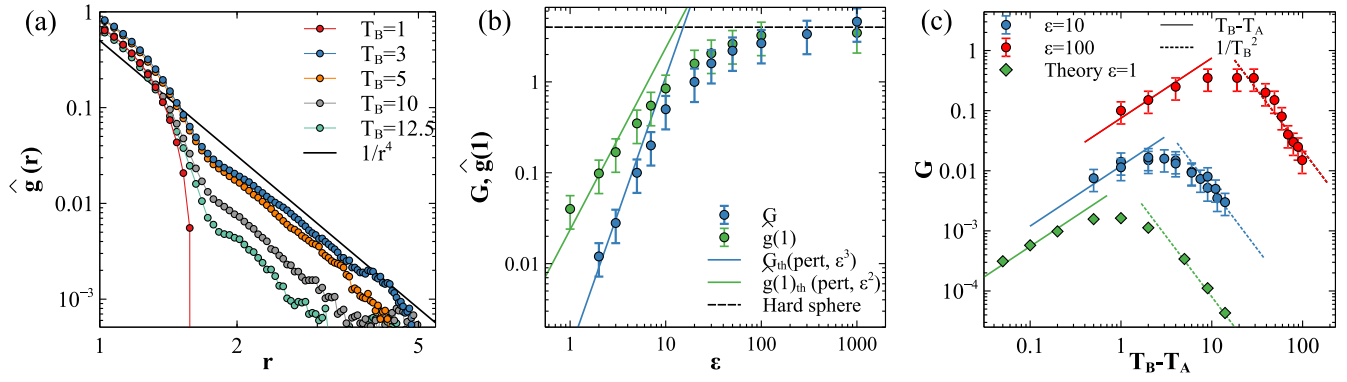

FIG. 1. (a) Correlation function $\hat{g}(r)$ of the species A for $T_A = 1$, $\epsilon = 10$, and $\rho = 0.05$ (T_B as indicated). (b) Correlation at contact $\hat{g}(1)$ and prefactor of the algebraic decay G as a function of ϵ ($T_A = 1$, $T_B = 3$). The solid lines correspond to the theoretical predictions. (c) Prefactor of the algebraic decay G as a function of $T_B - T_A$ and theoretical prediction (ϵ as indicated).

temperatures [Fig. 1(c)]. The temperature where the effect is maximal increases with the interaction strength ϵ. We now return to theory to (i) elucidate the discrepancy between the two arguments adapted out of equilibrium and (ii) find the origin and the characteristics of the algebraic decay.

We use two theoretical approaches. First, we use stochastic density field theory (SDFT) [34] to turn the microscopic dynamics (1) into exact Langevin equations for the density fields $\hat{\rho}_\alpha(\boldsymbol{x}, t) = \sum_{i \in I_\alpha} \delta(\boldsymbol{x} - \boldsymbol{x}_i(t))$, where $\alpha \in \{A, B\}$ indicate the species and I_α is the set of indices of the particles of species α. SDFT applies in equilibrium as well as in out-of-equilibrium situations [10,35,36]. The exact dynamics of the density fields is nonlinear due to pair interactions, and contains multiplicative noise, which makes it intractable in practical situations. In the limit of a dense system with weak interactions, SDFT can be linearized and the density fluctuations around the average densities ρ_α become Gaussian [37,38]; this approximation corresponds to the random phase approximation in liquid theory [30]. The correlation, which corresponds to the correlations of the fluctuations of the density fields, can be calculated in Fourier space [32]. In the dilute limit that we consider here ($\rho_A = 0$, $\rho_B \to 0$), it reduces to

$$\hat{g}(r) = \frac{V * V(r)}{T_A T_{AB}} + \mathcal{O}(\epsilon^3). \tag{9}$$

This expression is in quantitative agreement with the simulations for $r \lesssim 2$ (Supplemental Material, Fig. S3 [32]). It takes a similar form as the results obtained by adapting equilibrium arguments [Eqs. (6) and (8)], but the temperatures enter differently in the prefactor. As the expression (9) is exact at the order ϵ^2, we conclude that none of the two equilibrium calculations can be adapted out of equilibrium.

Yet, expression (9) vanishes at two particle diameters and does not explain the algebraic decay observed in the simulations [Fig. 1(a)]. This is expected, because the simulations indicate that the algebraic decay arises at order ϵ^3, while Eq. (9) is limited to order ϵ^2. We now turn to a small density expansion that is valid for any interaction strength. The N-particle distribution $f(\boldsymbol{X})$ is stationary under the Smoluchowski equation describing the microscopic dynamics (1):

$$\partial_t f = \sum_i \nabla_i \cdot \left[T_i \nabla_i f(\boldsymbol{X}) + f(\boldsymbol{X}) \sum_{j \neq i} \nabla V_{ij}(\boldsymbol{x}_i - \boldsymbol{x}_j) \right]. \tag{10}$$

To isolate the many-body effects from the pair correlation obtained by Grosberg and Joanny [18], we write it as

$$f(\boldsymbol{X}) = \exp\left(-\sum_{\langle ij \rangle} v_{ij} - \phi(\boldsymbol{X}) \right), \tag{11}$$

where now $v_{ij} = V(\boldsymbol{x}_i - \boldsymbol{x}_j)/T_{ij}$. The resulting equation for the many-body potential $\phi(\boldsymbol{X})$ is [32]

$$\begin{aligned} 0 = & \sum_i T_i [(\nabla_i \phi)^2 - \nabla_i^2 \phi] \\ & + \sum_{\langle ij \rangle} \nabla v_{ij} \cdot [(T_{ij} + \tau_{ij}) \nabla_i \phi - (T_{ij} - \tau_{ij}) \nabla_j \phi] \\ & + \sum_{\langle ijk \rangle} (\tau_{ijk} \nabla v_{ij} \cdot \nabla v_{ik} + \text{perm}), \end{aligned} \tag{12}$$

where we have defined the temperature differences $\tau_{ij} = T_i - T_j$ and $\tau_{ijk} = T_i - T_{jk}$ and "perm" indicates the two terms in the last sum obtained from the first by cyclic permutations. The third term is the source term: it is a sum over triplets, underlining the fact that ϕ originate from three-body effects. Moreover, it involves temperature differences so that it is zero at equilibrium. While this is expected, it stresses the fact that the N-particle distribution can be written as a product of pair terms only at equilibrium, and that three-body effects arise as soon as the system is put out of equilibrium, as evidenced for particles attached by linear springs [29]. Equation (12) for ϕ is a nonlinear

partial differential equation with multiplicative terms, and we solve it perturbatively in the interaction strength ϵ: we write $\phi = \sum_{k=2}^{\infty} \phi^{(k)}$, with $\phi^{(k)} \propto \epsilon^k$.

The depletion interaction encoded in $\hat{g}(r)$ can be computed from the three-body distribution $f(\boldsymbol{x}_1, \boldsymbol{x}_2, \boldsymbol{x}_3)$. Expanding f in powers of ϵ and integrating over $\boldsymbol{x}_3$, we find [32]

$$\hat{g} = \int \mathrm{d}\boldsymbol{x}_3 \Big[v_{13} v_{23} - \phi^{(2)} - \frac{1}{2}(v_{13}^2 v_{23} + v_{13} v_{23}^2) + (v_{13} + v_{23})\phi^{(2)} - \phi^{(3)} \Big] + \mathcal{O}(\epsilon^4). \tag{13}$$

The first two terms in the integrand are of order ϵ^2, while the last three are of order ϵ^3.

At order ϵ^2, the Laplacian in the first term balances the source term, and the solution is given by $\phi^{(2)}(\boldsymbol{X}) = \sum_{\langle ijk \rangle} \tau_{ijk} \omega_{ijk}^{(2)}(\boldsymbol{x}_j - \boldsymbol{x}_i, \boldsymbol{x}_k - \boldsymbol{x}_i) + \text{perm}$, where $\omega_{ijk}^{(2)}$ is given in Fourier space by [32]

$$\tilde{\omega}_{ijk}^{(2)}(\boldsymbol{k}, \boldsymbol{k}') = \frac{\boldsymbol{k} \cdot \boldsymbol{k}' \tilde{v}_{ij}(\boldsymbol{k}) \tilde{v}_{ik}(\boldsymbol{k}')}{2(T_i k^2 + T_{ik} k'^2 + T_i \boldsymbol{k} \cdot \boldsymbol{k}')}. \tag{14}$$

Using $\phi^{(2)}$ to compute $\hat{g}(r)$ at order ϵ^2, the expression (9) obtained from SDFT is recovered [32]. This result shows that the three-body effects are important to get the correct depletion interaction at order ϵ^2, and that these effects are included in the SDFT calculation.

To find $\phi^{(3)}$, we keep the terms of order ϵ^3 in Eq. (12):

$$\sum_i T_i \nabla_i^2 \phi^{(3)} = \sum_{\langle ij \rangle} \nabla v_{ij} \cdot [(T_{ij} + \tau_{ij}) \nabla_i \phi^{(2)} - (T_{ij} - \tau_{ij}) \nabla_j \phi^{(2)}], \tag{15}$$

which can be solved using the expression of $\phi^{(2)}$ obtained previously [32]. Using $\phi^{(2)}$ and $\phi^{(3)}$ in the correction (13) leads the depletion interaction at order ϵ^3. The resulting expression contains many terms involving double integrals in Fourier space, which can be performed numerically, yielding a good agreement with the $\hat{g}(r)$ obtained from simulations (Fig. S3 [32]). The small wave-vector behavior in Fourier space leads to an algebraic decay:

$$\hat{g}(r) \underset{r \to \infty}{\sim} G_U\left(\frac{e}{T_A}, \frac{T_B}{T_A}\right) r^{-2d}, \tag{16}$$

where

$$G_U(e, \theta) \underset{e \to 0}{\sim} [e \tilde{U}(0)]^3 F(\theta). \tag{17}$$

This prediction agrees quantitatively with the simulations for the harmonic and Gaussian interactions, which are integrable (Fig. 2). The temperature dependence follows

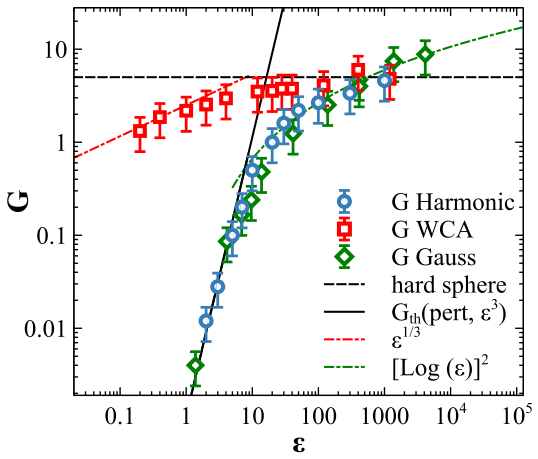

FIG. 2. Prefactor G of the algebraic decay as a function of the interaction strength ϵ for the harmonic (blue circles), Gaussian (green diamonds), and WCA (red squares) interactions from the numerical simulations. The lines represent the several asymptotic expressions: weak interaction for an integrable potential (black solid line), hard spheres (black dashed line), weak interaction for a WCA potential (red dash-dotted line) and strong interaction from a Gaussian interaction (green dash-dotted line).

$F(\theta) \sim \theta - 1$ close to equilibrium ($\theta \to 1$), consistent with the fact that the algebraic interaction emerges from the temperature differences. When the B particles are very hot ($\theta \to \infty$), they are barely affected by the interactions and the prefactor decays as $F(\theta) \sim \theta^{-2}$. These behaviors are confirmed by the simulations [Fig. 1(c)].

Furthermore, the simulations show that the algebraic decay as r^{-2d} holds for the three different interactions, harmonic, WCA, Gaussian, independently of their strength [Figs. S4(a) and S4(b) [32]]. Hard spheres are obtained as the strong interaction limit for interactions with a finite range σ. In this limit, the prefactor depends only on the diameter σ (Fig. 2). Assuming that the correlation depends only on the dimensionless ratio r/σ, the prefactor should thus be

$$G_U(e, \theta) \underset{e \to \infty}{\to} \sigma^{2d} F_{\mathrm{hs}}(\theta); \tag{18}$$

this argument is confirmed by simulations [Fig. S4(c) [32]]. Two situations remain uncovered by the analysis above: the WCA interaction in the soft limit, because it is not integrable, and the Gaussian interaction in the hard limit, because its range is not finite. They can be addressed by defining the effective diameter σ_{eff} as $\epsilon U(\sigma_{\mathrm{eff}}) = T_A$, and then using it as an effective hard sphere diameter. For the WCA interaction in the limit $\epsilon \to 0$, this gives $\sigma_{\mathrm{eff}}^{\mathrm{WCA}} \sim (\epsilon/T_A)^{1/12}$ and $G_U(e, \theta) \sim e^{1/3}$. For the Gaussian interaction in the limit $\epsilon \to \infty$, this gives $\sigma_{\mathrm{eff}}^{\mathrm{Gauss}} \sim \sqrt{\log(\epsilon/T_A)}$ and $G_U(e, \theta) \sim [\log(e)]^2$. These behaviors are compatible with the simulations (Fig. 2). Finally, we ran numerical simulations with a Lennard-Jones interaction, which has an

attractive part. Two behaviors are observed: if the attraction is small enough, the system remains homogeneous and the algebraic decay of the correlation is observed; if the attraction is too strong, the cold particles aggregate and the algebraic decay is lost (Fig. S5 [32]).

The depletion interaction that we have unveiled is the driving force behind the formation of dense droplets of cold particles when they separate from the hot particles. As the algebraic tail of the interaction originates from temperature differences [τ_{ijk} in Eq. (12)], this effect is reversed if one considers the depletion interaction induced by the cold particles on the hot ones, so that the algebraic tail is *repulsive* in this case. This repulsion between hot particles may work with the attraction between cold particles to trigger the phase separation. Our results may also apply to mixtures of passive and artificial [39,40] or living [41,42] self-propelled particles, which could be described at large scales by two-temperature mixtures.

Acknowledgments—The authors acknowledge fruitful discussions with Denis Dumont and Cesare Nardini and the support by FRS-FNRS under Research Grant (PDR "Active Matter in Harmonic Trap") No. T.0251.20. This work was supported by the Belgian National Fund for Scientific Research (FRS-FNRS) within the Consortium des équipements de Calcul Intensif–CECI, under Grant No. 2.5020.11t. Q. T. received support as a FRIA grant holder from the Belgian National Fund for Scientific Research (FRS-FNRS).

[1] H. B. G. Casimir, On the attraction between two perfectly conducting plates, Proc. R. Neth. Acad. Arts Sci. **51**, 793 (1948).
[2] A. O. Sushkov, W. J. Kim, D. A. R. Dalvit, and S. K. Lamoreaux, Observation of the thermal Casimir force, Nat. Phys. **7**, 230 (2011).
[3] M. E. Fisher and P.-G. de Gennes, Phénomènes aux parois dans un mélange binaire critique, C. R. Seances Acad. Sci. **287**, 207 (1978).
[4] C. Hertlein, L. Helden, A. Gambassi, S. Dietrich, and C. Bechinger, Direct measurement of critical Casimir forces, Nature (London) **451**, 172 (2008).
[5] A. Maciołek and S. Dietrich, Collective behavior of colloids due to critical Casimir interactions, Rev. Mod. Phys. **90**, 045001 (2018).
[6] S. Mahdisoltani and R. Golestanian, Long-range fluctuation-induced forces in driven electrolytes, Phys. Rev. Lett. **126**, 158002 (2021).
[7] S. Mahdisoltani and R. Golestanian, Transient fluctuation-induced forces in driven electrolytes after an electric field quench, New J. Phys. **23**, 073034 (2021).
[8] G. Du, D. S. Dean, B. Miao, and R. Podgornik, Correlation decoupling of Casimir interaction in an electrolyte driven by external electric fields, Phys. Rev. Lett. **133**, 238002 (2024).
[9] T. Vissers, A. Wysocki, M. Rex, H. Lowen, C. P. Royall, A. Imhof, and A. van Blaaderen, Lane formation in driven mixtures of oppositely charged colloids, Soft Matter **7**, 2352 (2011).
[10] A. Poncet, O. Bénichou, V. Démery, and G. Oshanin, Universal long ranged correlations in driven binary mixtures, Phys. Rev. Lett. **118**, 118002 (2017).
[11] C. M. Rohwer, M. Kardar, and M. Krüger, Transient Casimir forces from quenches in thermal and active matter, Phys. Rev. Lett. **118**, 015702 (2017).
[12] C. M. Rohwer, A. Solon, M. Kardar, and M. Krüger, Nonequilibrium forces following quenches in active and thermal matter, Phys. Rev. E **97**, 032125 (2018).
[13] L. Angelani, C. Maggi, M. L. Bernardini, A. Rizzo, and R. Di Leonardo, Effective interactions between colloidal particles suspended in a bath of swimming cells, Phys. Rev. Lett. **107**, 138302 (2011).
[14] Y. Baek, A. P. Solon, X. Xu, N. Nikola, and Y. Kafri, Generic long-range interactions between passive bodies in an active fluid, Phys. Rev. Lett. **120**, 058002 (2018).
[15] O. Granek, Y. Baek, Y. Kafri, and A. P. Solon, Bodies in an interacting active fluid: Far-field influence of a single body and interaction between two bodies, J. Stat. Mech. Theory Exp. **2020**, 063211 (2020).
[16] G. Fava, A. Gambassi, and F. Ginelli, Strong Casimir-like forces in flocking active matter, Phys. Rev. Lett. **133**, 148301 (2024).
[17] A. Awazu, Segregation and phase inversion of strongly and weakly fluctuating Brownian particle mixtures and a chain of such particle mixtures in spherical containers, Phys. Rev. E **90**, 042308 (2014).
[18] A. Y. Grosberg and J. F. Joanny, Nonequilibrium statistical mechanics of mixtures of particles in contact with different thermostats, Phys. Rev. E **92**, 032118 (2015).
[19] S. N. Weber, C. A. Weber, and E. Frey, Binary mixtures of particles with different diffusivities demix, Phys. Rev. Lett. **116**, 058301 (2016).
[20] S. R. McCandlish, A. Baskaran, and M. F. Hagan, Spontaneous segregation of self-propelled particles with different motilities, Soft Matter **8**, 2527 (2012).
[21] J. Stenhammar, R. Wittkowski, D. Marenduzzo, and M. E. Cates, Activity-induced phase separation and self-assembly in mixtures of active and passive particles, Phys. Rev. Lett. **114**, 018301 (2015).
[22] L. Abbaspour, R. Mandal, P. Sollich, and S. Klumpp, Long-range velocity correlations from active dopants, Commun. Phys. **7**, 289 (2024).
[23] R. Soto and R. Golestanian, Self-assembly of catalytically active colloidal molecules: Tailoring activity through surface chemistry, Phys. Rev. Lett. **112**, 068301 (2014).
[24] A. V. Ivlev, J. Bartnick, M. Heinen, C.-R. Du, V. Nosenko, and H. Löwen, Statistical mechanics where Newton's third law is broken, Phys. Rev. X **5**, 011035 (2015).
[25] Y. Duan, J. Agudo-Canalejo, R. Golestanian, and B. Mahault, Dynamical pattern formation without self-attraction in quorum-sensing active matter: The interplay between nonreciprocity and motility, Phys. Rev. Lett. **131**, 148301 (2023).
[26] E. Ilker and J.-F. Joanny, Phase separation and nucleation in mixtures of particles with different temperatures, Phys. Rev. Res. **2**, 023200 (2020).

[27] E. McCarthy, R. K. Manna, O. Damavandi, and M. L. Manning, Demixing in binary mixtures with differential diffusivity at high density, Phys. Rev. Lett. **132**, 098301 (2024).
[28] A. P. Solon, Y. Fily, A. Baskaran, M. E. Cates, Y. Kafri, M. Kardar, and J. Tailleur, Pressure is not a state function for generic active fluids, Nat. Phys. **11**, 673 (2015).
[29] M. Wang and A. Y. Grosberg, Three-body problem for Langevin dynamics with different temperatures, Phys. Rev. E **101**, 032131 (2020).
[30] J.-P. Hansen and I. R. McDonald, *Theory of Simple Liquids*, 3rd ed. (Academic Press, London, 2006).
[31] Y. Mao, M. Cates, and H. Lekkerkerker, Depletion force in colloidal systems, Phys. A **222**, 10 (1995).
[32] See Supplemental Material at http://link.aps.org/supplemental/10.1103/PhysRevLett.133.267103 for supplementary figures, methods, and calculations.
[33] A. P. Thompson, H. M. Aktulga, R. Berger, D. S. Bolintineanu, W. M. Brown, P. S. Crozier, P. J. in 't Veld, A. Kohlmeyer, S. G. Moore, T. D. Nguyen, R. Shan, M. J. Stevens, J. Tranchida, C. Trott, and S. J. Plimpton, LAMMPS—A flexible simulation tool for particle-based materials modeling at the atomic, meso, and continuum scales, Comput. Phys. Commun. **271**, 108171 (2022).
[34] D. S. Dean, Langevin equation for the density of a system of interacting Langevin processes, J. Phys. A Math. Gen. **29**, L613 (1996).
[35] V. Démery and D. S. Dean, The conductivity of strong electrolytes from stochastic density functional theory, J. Stat. Mech. Theory Exp. **2016**, 023106 (2016).
[36] A. Benois, M. Jardat, V. Dahirel, V. Démery, J. Agudo-Canalejo, R. Golestanian, and P. Illien, Enhanced diffusion of tracer particles in nonreciprocal mixtures, Phys. Rev. E **108**, 054606 (2023).
[37] V. Démery, O. Bénichou, and H. Jacquin, Generalized Langevin equations for a driven tracer in dense soft colloids: Construction and applications, New J. Phys. **16**, 053032 (2014).
[38] D. S. Dean and R. Podgornik, Relaxation of the thermal Casimir force between net neutral plates containing Brownian charges, Phys. Rev. E **89**, 032117 (2014).
[39] D. P. Singh, U. Choudhury, P. Fischer, and A. G. Mark, Non-equilibrium assembly of light-activated colloidal mixtures, Adv. Mater. **29**, 1701328 (2017).
[40] I. P. Madden, L. Wang, J. Simmchen, and E. Luijten, Hydrodynamically controlled self-organization in mixtures of active and passive colloids, Small **18**, 2107023 (2022).
[41] L. Ortlieb, S. Rafaı, P. Peyla, C. Wagner, and T. John, Statistics of colloidal suspensions stirred by microswimmers, Phys. Rev. Lett. **122**, 148101 (2019).
[42] A. Lagarde, N. Dagès, T. Nemoto, V. Démery, D. Bartolo, and T. Gibaud, Colloidal transport in bacteria suspensions: From bacteria collision to anomalous and enhanced diffusion, Soft Matter **16**, 7503 (2020).